COMSOL CONFERENCE
2019 BOSTON

Phase Field Modelling of Gas Migration in Bentonite Based Barrier Materials

Presenter: Guanlong Guo

Supervisor: Mamadou Fall

Department of Civil Engineering, University of Ottawa, Canada

Date: 3/10/2019

OUTLINE

1. Introduction
2. Conceptual Coupled HM-PF Model
3. Numerical Implementation
4. Simulation Results
5. Conclusions

1 Introduction

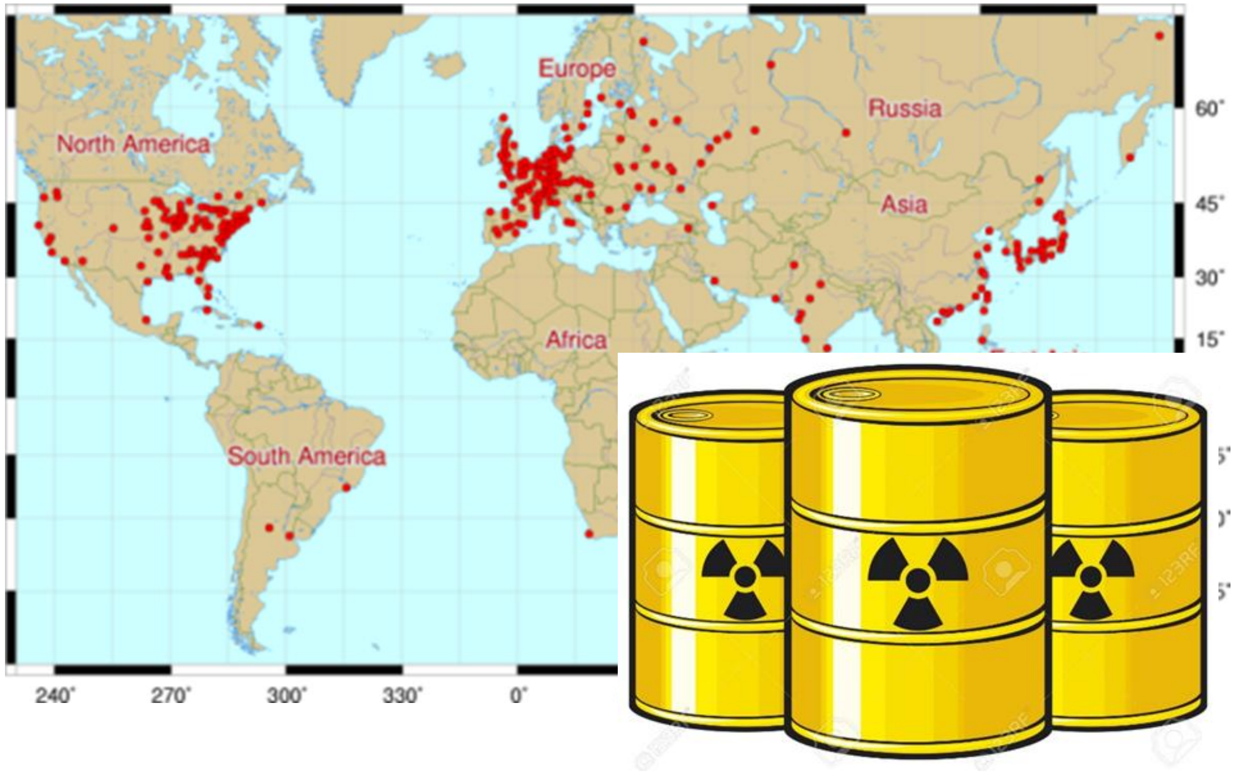

Distribution of Nuclear Power Plants
(From Wikipedia)

1 Introduction

Engineering Barrier System

Natural Barrier System

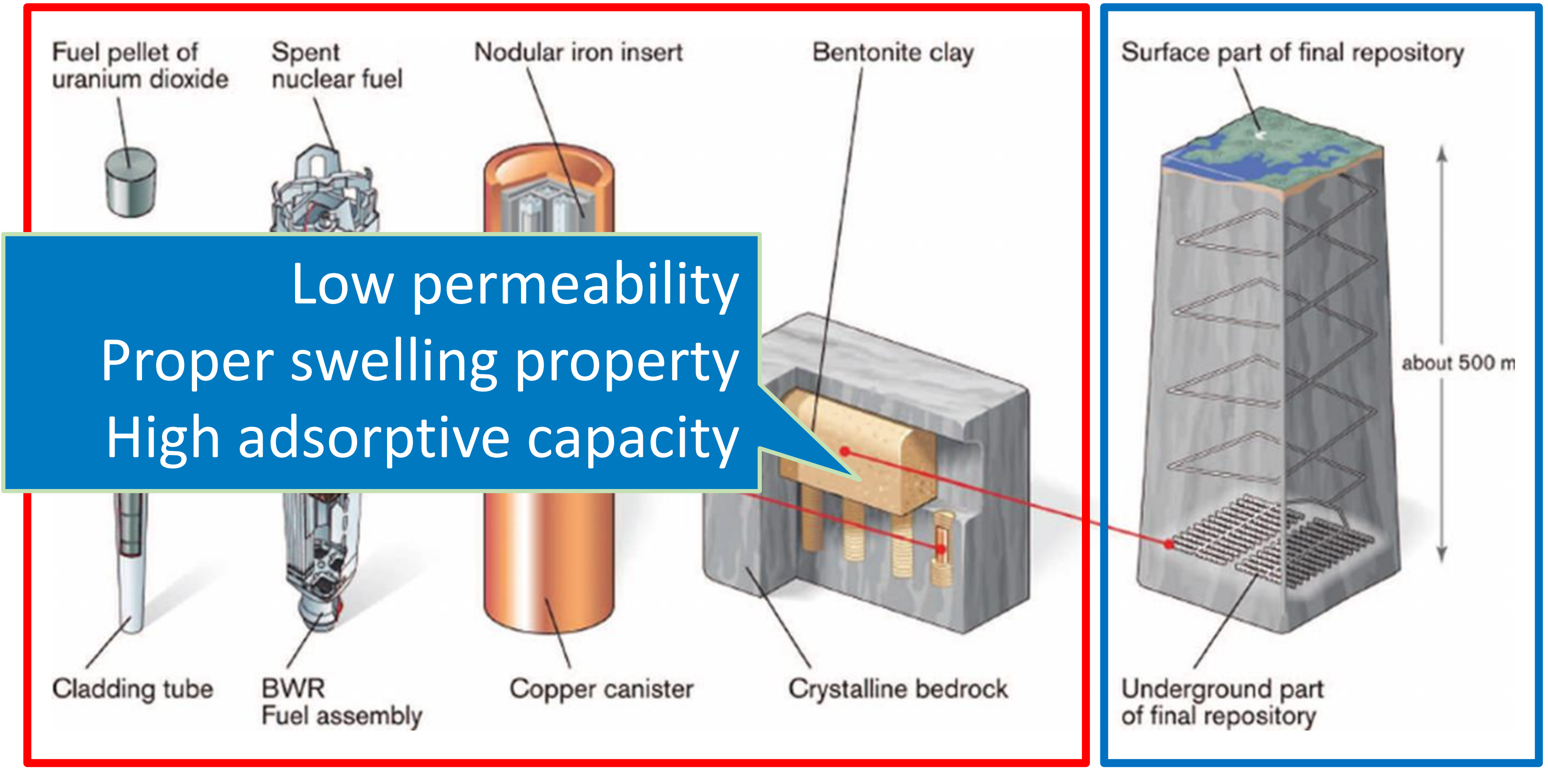

Multi-barrier system of KBS-3 repository

(From Harrington, J., and Horseman, S. 2003)

Metal Corrosion

Water Radiolysis

Bio-Degradation

Gas Generation

Gas Transport

0 → P_g

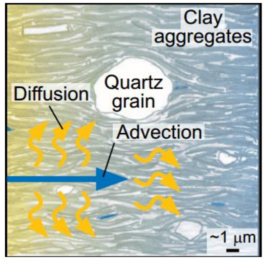

Gas Diffusion

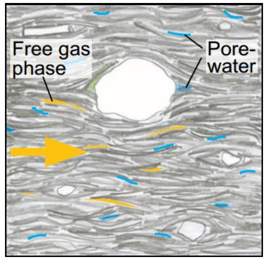

Two Phase Flow

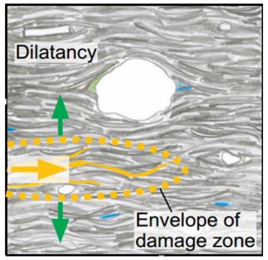

Dilatancy Control Flow

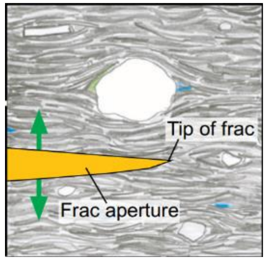

Macro-fracture Flow

*Images from Marschall et al. (2005)

2 Conceptual Coupled HM-PF Model

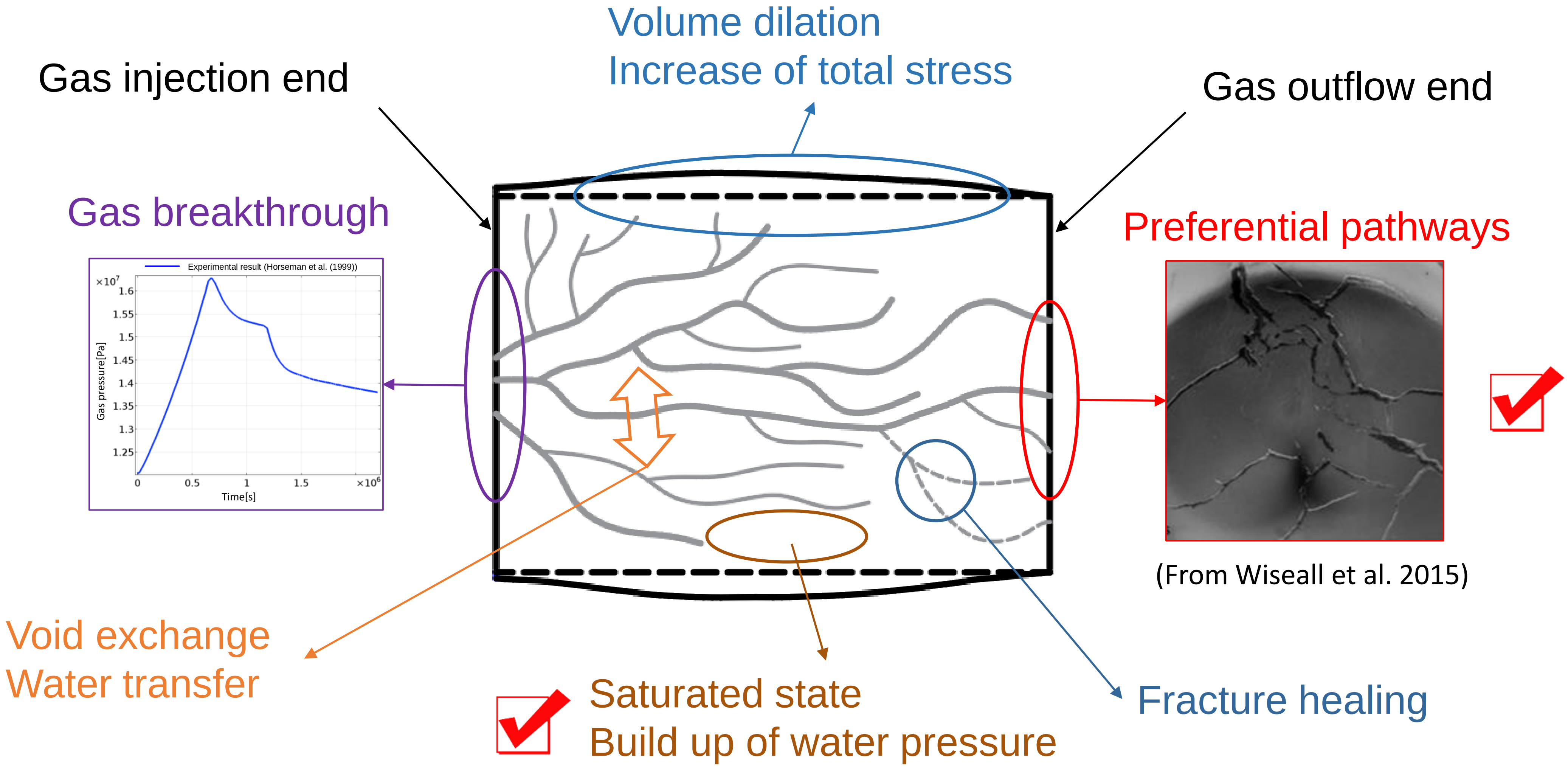

➢ Couplings Between Different Physical Field

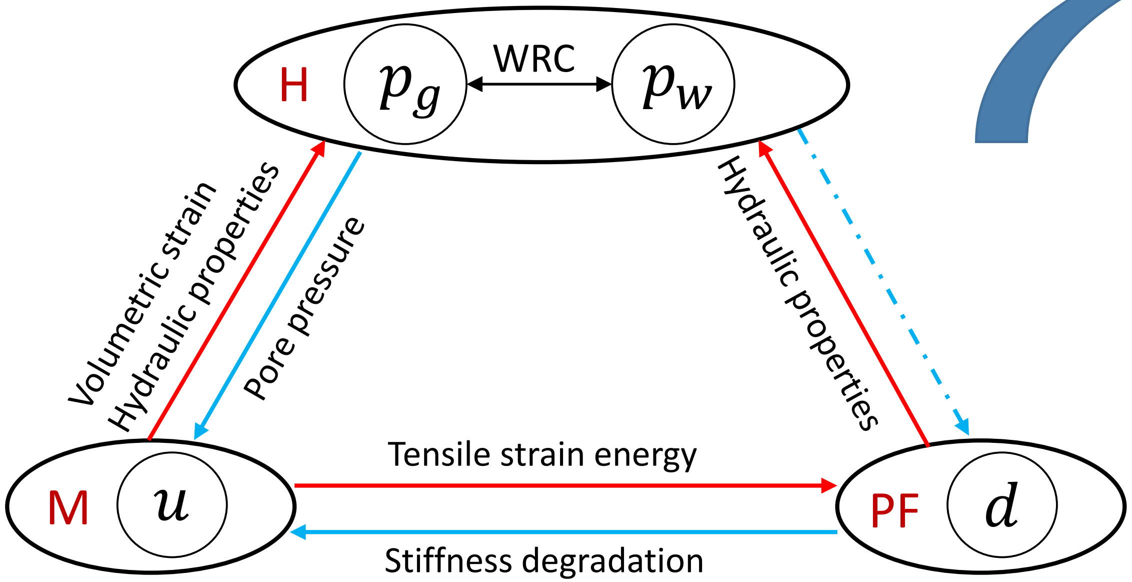

(Modified from Guo, G. & Fall, M. 2019)

3 Numerical Model and Implementation

➢ Phase Field Method

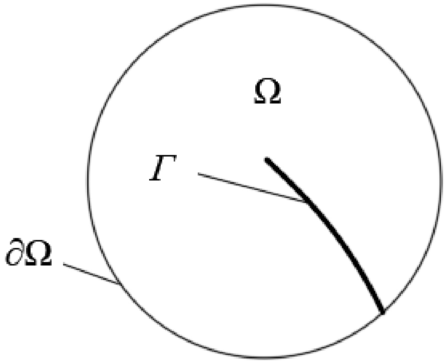

$$\gamma(d,\nabla d)=\frac{1}{2l}d^2+\frac{l}{2}|\nabla d|^2$$

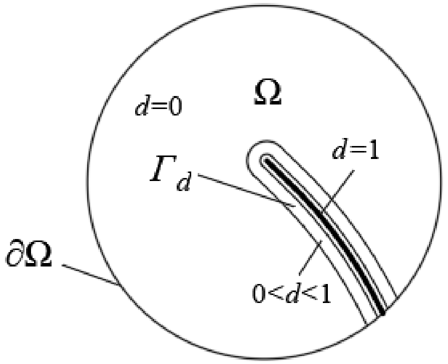

Variational Principle of Free Energy Minimization

$$(1-d)H_M^+-\left(d-l^2\nabla^2 d\right)=0 \qquad H_M^+=\max_{\tau\in[0,t]}\left\{\left\langle\frac{\psi_0^{e+}}{\psi_{cr}}-1\right\rangle_+\right\}$$

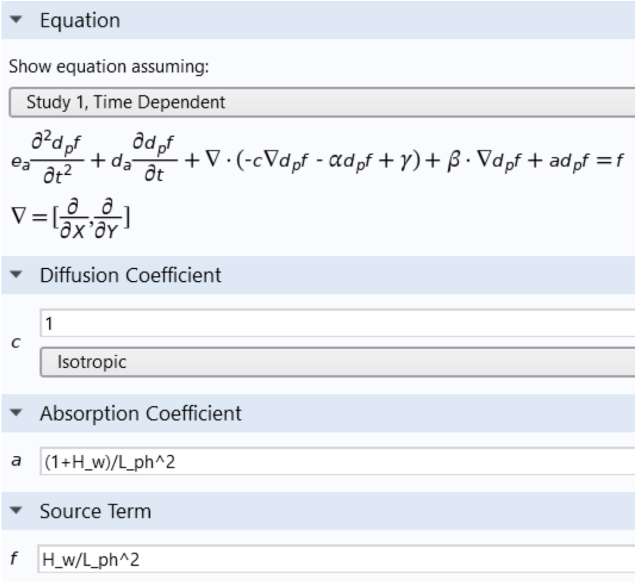

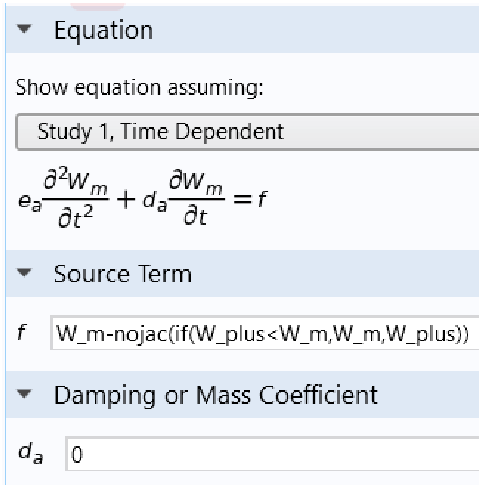


Previous Solution 1

➢ Mechanical Model

- Solid Mechanics *(fcon)*
  - Linear Elastic Material 1
    - External Stress 1
    - Initial Stress and Strain 1
    - Equation View

$$\nabla\cdot\left[g(d)\boldsymbol{\sigma}'^{+}(\boldsymbol{\varepsilon})+\boldsymbol{\sigma}'^{-}(\boldsymbol{\varepsilon})-\bar{p}\boldsymbol{I}\right]+\rho\boldsymbol{g}=\boldsymbol{0}$$

External Stress

Stress input:

Pore pressure

Absolute pressure:

p_A User defined

p_ave

$$\boldsymbol{\sigma}'^{\pm}(\boldsymbol{\varepsilon})=\sum_{a=1}^{3}\left[\lambda\langle tr(\boldsymbol{\varepsilon})\rangle_{\pm}+2\mu\langle\varepsilon_a\rangle_{\pm}\right]\boldsymbol{n}_a\otimes\boldsymbol{n}_a$$

- Solid Mechanics *(fcon)*
  - Linear Elastic Material 1
    - External Stress 1
    - Initial Stress and Strain 1
    - Equation View

- Strain
  - Principal strain directions
    - Principal strain direction 1 (material and geometry frames)
    - Principal strain direction 2 (material and geometry frames)
    - Principal strain direction 3 (material and geometry frames)

Replace

	fcon.Jel	sqrt(fcon.Cel11*fcon.Cel22*fcon.C...	1
	fcon.Sl11	fcon.Sil11+fcon.D11*fcon.eel11+f...	N/m²
	fcon.Sl12	fcon.Sil12+fcon.D14*fcon.eel11+f...	N/m²
	fcon.Sl13	fcon.Sil13+fcon.D16*fcon.eel11+f...	N/m²
	fcon.Sl22	fcon.Sil22+fcon.D12*fcon.eel11+f...	N/m²
	fcon.Sl23	fcon.Sil23+fcon.D15*fcon.eel11+f...	N/m²
	fcon.Sl33	fcon.Sil33+fcon.D13*fcon.eel11+f...	N/m²

- Principal strains
  - fcon.ep1 - First principal strain
  - fcon.ep2 - Second principal strain
  - fcon.ep3 - Third principal strain

➢ Hydraulic Model

$$\mathbf{v}_\kappa^D = -\frac{k_{in}k_{r\kappa}}{\mu_\kappa}\left(\nabla p_\kappa - \rho_\kappa \mathbf{g}\right)$$

$$\rho_\kappa \phi \underbrace{\left(\frac{S_\kappa}{K_\kappa} - \frac{\partial S_e}{\partial p_c}\right)}_{S}\frac{\partial p_\kappa}{\partial t} + \nabla\cdot\left(\rho_\kappa \mathbf{v}_\kappa^D\right)$$

$$= \underbrace{-S_\kappa \rho_\kappa \frac{\partial \varepsilon_v}{\partial t} - \rho_\kappa \phi \frac{\partial S_e}{\partial p_c}\frac{\partial p_{\kappa'}}{\partial t}}_{Q}$$

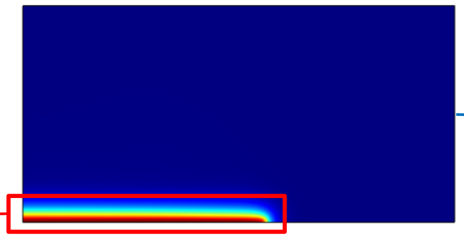

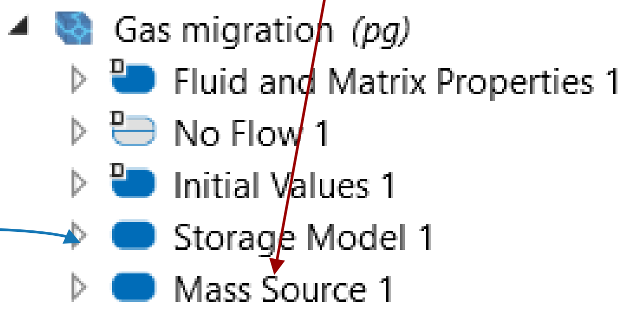

$$\mathbf{k}_{fin} = C_k \mathbf{k}_{pin}$$ *

$$k_{frw} = \frac{1}{2}S_w^2\left(3 - S_w\right)$$

$$k_{frg} = S_g^3 + \frac{3}{2M}S_g\left(1 - S_g^2\right)$$

$$S_{fe} = \left[1 + \left(\frac{p_c}{p_{fgev}}\right)^n\right]^{-m}$$

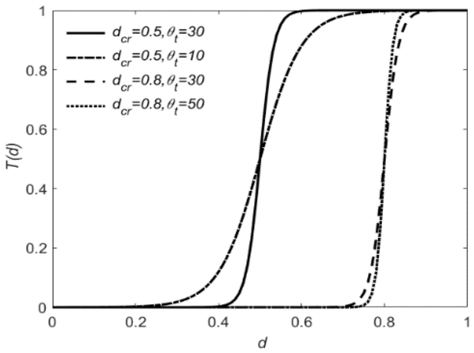

Transition function

$$k_{pin}$$ *

$$k_{prw} = \sqrt{S_e}\left[1 - \left(1 - S_e^{1/m}\right)^m\right]^2$$

$$k_{prg} = \sqrt{1 - S_e}\left(1 - S_e^{1/m}\right)^{2m}$$

$$S_{pe} = \left[1 + \left(\frac{p_c}{p_{pgev}}\right)^n\right]^{-m}$$

$$T(d) = \frac{1}{2}\left\{\tanh\left[\theta_t\left(d - d_{cr}\right)\right] - \tanh\left(-d_{cr}\theta_t\right)\right\}$$

* (From Guo, G. & Fall, M. 2019)

➢ Solver Settings

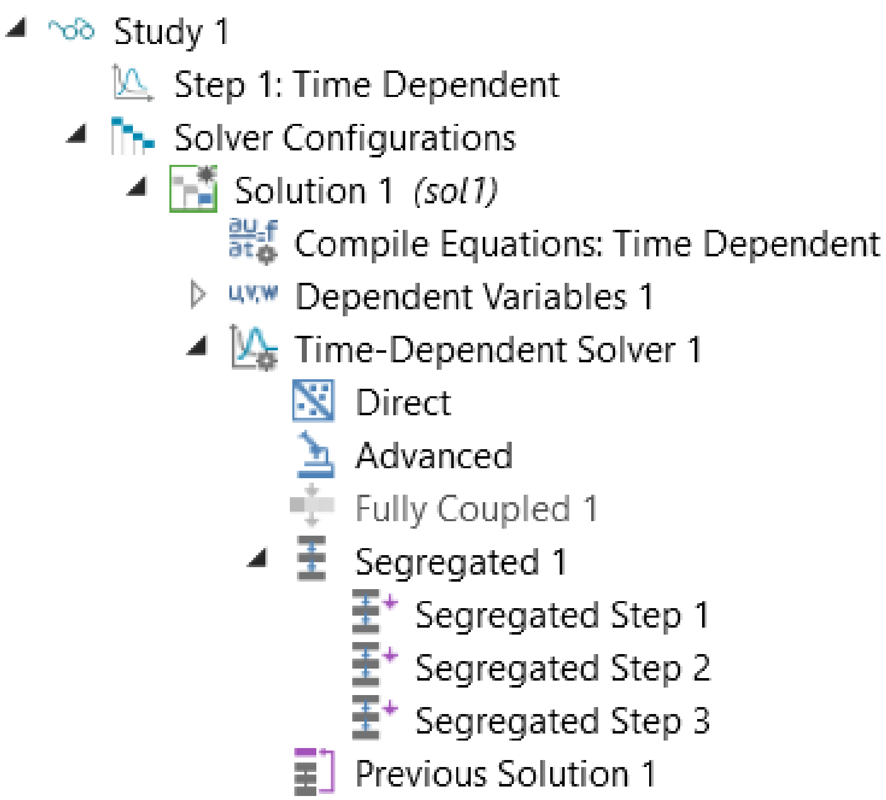

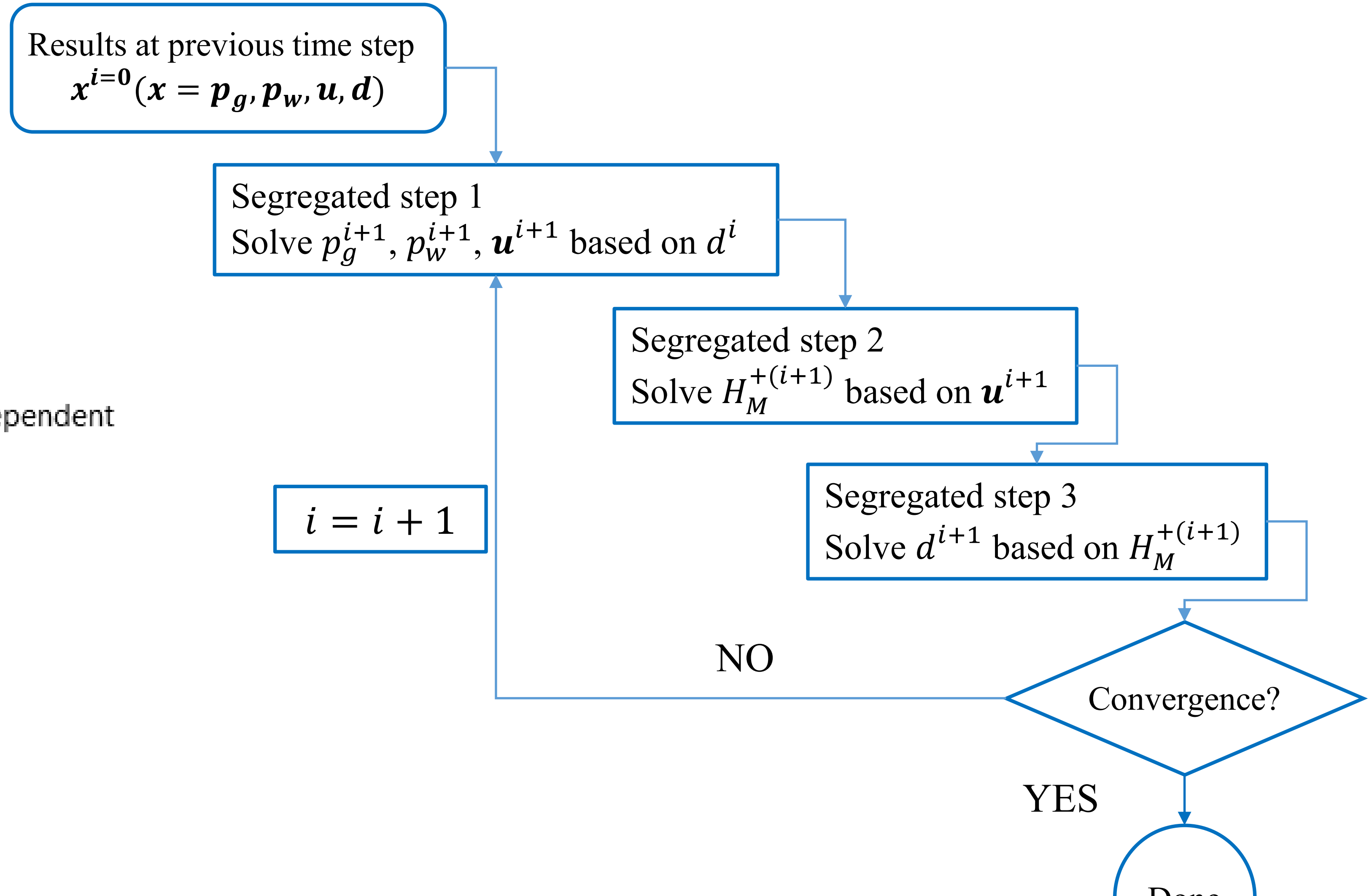

(Modified from https://www.comsol.com/blogs/improving-convergence-multiphysics-problems/)

4 Simulation Results

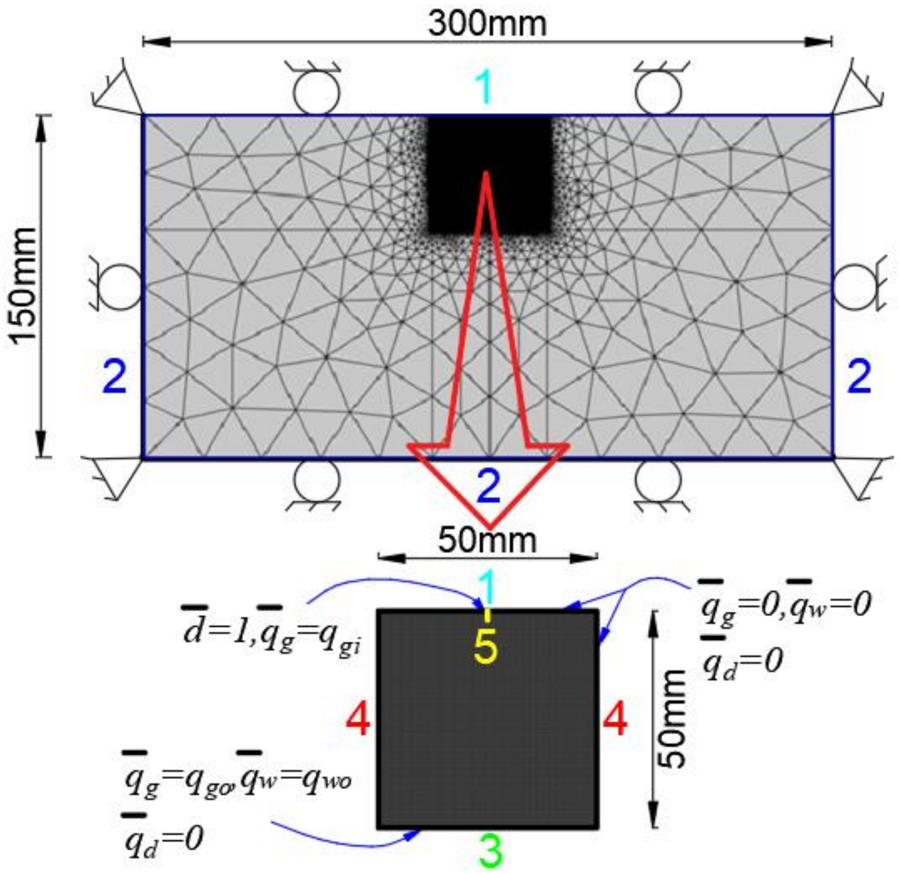

➢ Meshing and boundary conditions

(Modified from Guo, G. & Fall, M. 2019)

Preferentially propagate through areas of low resistance

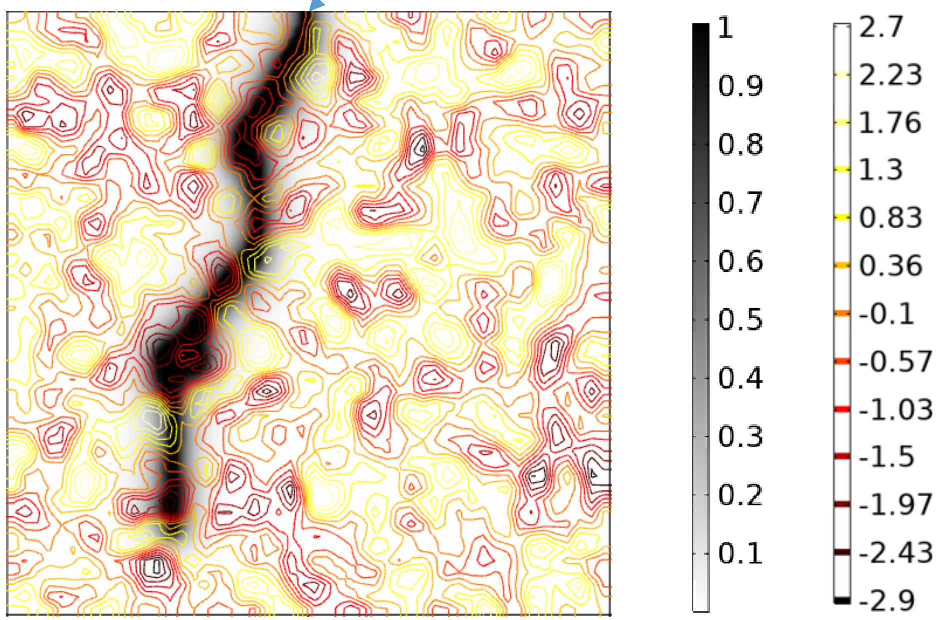

➢ Fracture trajectory (Phase field) in the heterogeneous domain

Preferential gas flow in the developed fracture

Rise of water pressure during fracturing process

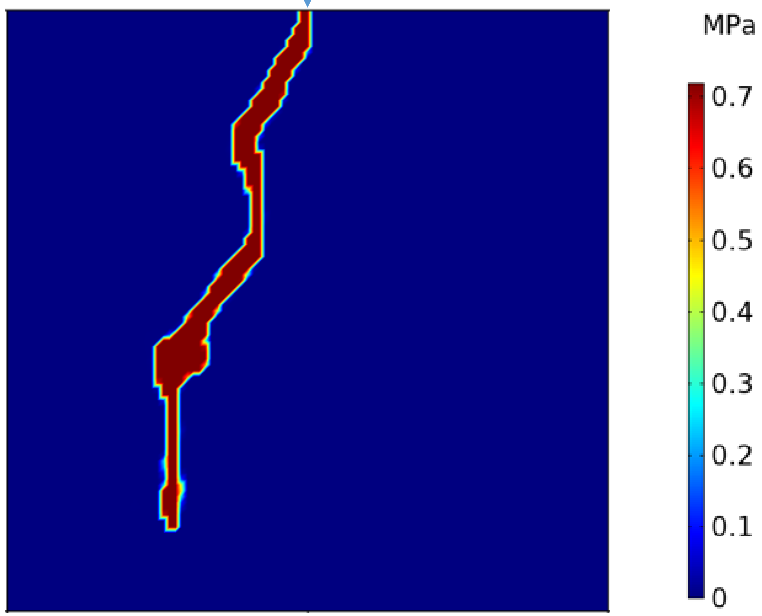

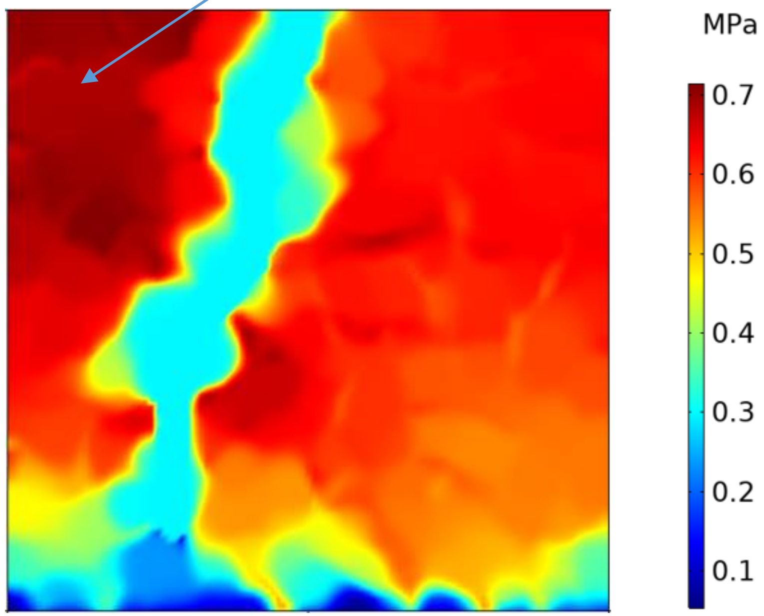

- Distribution of gas pressure (scaled by its degree of saturation)
- Distribution of water pressure

4 Conclusions

- The developed coupled HM-PF model is successfully implemented into COMSOL by using Solid Mechanics Module, Darcy’s Law Module, Coefficient Form PDE, Domain ODEs and DAEs and the Previous Solution Node.
- The developed model has satisfactorily described some HM behaviors observed in experiments, such as the development of preferential pathways, the localized gas flow and the rise of water pressure.

References

- Guo, G. & Fall, M. 2018. Modelling of dilatancy-controlled gas flow in saturated bentonite with double porosity and double effective stress concepts. Engineering Geology, 243, 253-271
- Guo, G. & Fall, M. 2019. Modelling of preferential gas flow in heterogeneous and saturated bentonite based on phase field method. Computers and Geotechnics, 116, 103206
- Harrington, J., and Horseman, S. 2003. Gas migration in KBS-3 buffer bentonite, Sensitivity of Test Parameters to Experimental Boundary Conditions Swedish Nuclear Fuel and Waste Management Company, Stockholm (Sweden).
- Horseman, S.T., Harrington, J.F., and Sellin, P. 1999. Gas migration in clay barriers, Engineering Geology 54(1-2): 139-149.
- Miehe, C., Welschinger, F., and Hofacker, M. 2010. Thermodynamically consistent phase-field models of fracture: Variational principles and multi-field FE implementations, International journal for numerical methods in engineering 83(10): 1273-1311.
- Miehe, C., Hofacker, M., and Welschinger, F. 2010. A phase field model for rate-independent crack propagation: Robust algorithmic implementation based on operator splits, Comput Method Appl M 199(45-48): 2765-2778.
- Mauthe, S. & Miehe, C. 2017. Hydraulic fracture in poro-hydro-elastic media. Mechanics Research Communications, 80, 69-83.
- Marschall, P., Horseman, S., and Gimmi, T. 2005. Characterisation of gas transport properties of the Opalinus Clay, a potential host rock formation for radioactive waste disposal, Oil & gas science and technology 60(1): 121-139.
- Wiseall, A., Cuss, R., Graham, C. & Harrington, J. 2015. The visualization of flow paths in experimental studies of clay-rich materials. Mineralogical Magazine, 79, 1335-1342.

Thank you for your attention!